

Substrate-Induced Growth of Nanostructured Zinc Oxide Films at Room Temperature Using Concepts of Biomimetic Catalysis

Birgit Schwenzer, John R. Gomm, and Daniel E. Morse*

Contribution from the California NanoSystems Institute, the Materials Research Laboratory, the Institute for Collaborative Biotechnologies, and the Department of Molecular, Cellular and Developmental Biology, University of California, Santa Barbara, Santa Barbara, California, 93106.

Received September 14, 2006

By kinetically controlled vapor-diffusion catalysis, nanostructured ZnO and $\text{Zn}_5(\text{OH})_8(\text{NO}_3)_3 \cdot 2\text{H}_2\text{O}$ thin films have been grown on substrates with different chemical compositions and varying degrees of crystallinity. The materials resulting from heterogeneous nucleation under mild conditions (starting from aqueous metal salt precursor solutions at room temperature) were characterized by X-ray diffraction and scanning electron microscopy to determine the influence of the substrates on the overall chemical composition, crystallinity, and morphology of the films.

1. Introduction

Zinc oxide (ZnO), one of the most important semiconducting materials, has been widely studied and used in numerous applications because of its unique combination of properties that include transparency, piezoelectric activity, and an optoelectronic band gap of 3.37 eV. ZnO thin films are currently fabricated by chemical vapor deposition (CVD), pulsed laser deposition (PLD), molecular beam epitaxy (MBE), chemical spray pyrolysis, or other high-temperature and in some cases capital- and equipment-intensive methods.¹ Innovations in the synthesis of ZnO nanostructures for field effect transistors and other electronic applications recently have been reported.^{2–5}

Using concepts that we translated from the molecular mechanism of biosilicification in marine sponges,^{6,7} we have successfully prepared nanostructured polycrystalline ZnO thin films on different substrates under environmentally benign conditions from an aqueous solution of precursor at room temperature. By diffusing ammonia vapor into an aqueous precursor solution, we use the concepts of slow catalysis and vectorial spatial control to prepare uniquely nanostructured metal hydroxide and metal oxide films. By changing the pH of the precursor solution slowly and in a vectorially directed manner, the diffusing ammonia establishes a gradient of catalyst concentration, providing a more detailed and spatially structured reaction environment than is obtained when employing solvothermal methods for nucleation of metal oxide films. As a result, the formation of crystallographic phases otherwise not attainable at low temperatures is facilitated. In contrast, although Hosono et al. recently reported the growth of nanostructured $\text{Zn}(\text{CO}_3)_x(\text{OH})_y \cdot n\text{H}_2\text{O}$ films on glass under mild solvothermal condition (3–48 h at 80 °C), their approach did not yield ZnO directly; the resulting films required conversion to ZnO by annealing in air at 300 °C.⁸

The work reported here is an extension of our recent studies of unsupported nanostructured metal hydroxide films grown by a biologically inspired, kinetically controlled synthesis method involving the vapor diffusion of a catalyst through the air–water interface of aqueous precursor solutions.⁹ Using this method, we previously reported the synthesis of unsupported, template-free $\text{Zn}_5(\text{OH})_8(\text{NO}_3)_2 \cdot 2\text{H}_2\text{O}$ ^{9,10} and ZnO¹¹ thin films, with nanostructured morphology on one side of the films, starting from aqueous $\text{Zn}(\text{NO}_3)_2$ precursor solutions at room temperature.

Films of hexagonal ZnO have previously been prepared by other research groups.^{8,12–14} In most cases however, slightly elevated temperatures and additives have been used for the preparation of ZnO films from aqueous solution^{12–14} or the as-grown films were converted to ZnO by subsequent annealing.⁸ In other cases, pretreatment of the underlying substrates was required to create a nucleation layer of a different material that promotes the growth of ZnO. Yamabi and Imai, for example, obtained good heterogeneous nucleation only after adjusting the pH and the $\text{Zn}(\text{NO}_3)_2$ /additive ratio and using a buffer layer of $\text{Zn}(\text{O}_2\text{CCH}_3)_2$ on substrates such as glass.¹⁴

2. Results and Discussion

We report here the effect on crystallinity and morphology of films grown by heterogeneous nucleation from aqueous $\text{Zn}(\text{NO}_3)_2$ when different substrates are introduced into the reaction system of the vapor-diffusion catalysis method. These substrates [amorphous glass, indium tin oxide coated glass (ITO), fluorine doped indium tin oxide (FTO), and ZnO (0001)] were selected for the differences in their crystallinity, crystallographic lattice matching with respect to ZnO and $\text{Zn}_5(\text{OH})_8(\text{NO}_3)_2 \cdot 2\text{H}_2\text{O}$, and polycrystalline or epitaxially grown surface morphologies. For amorphous glass, no lattice match is assumed. For the substrates coated with tetragonal polycrystalline ITO and FTO ($a = b = 4.720(0)$ Å and $c = 3.170(0)$ Å¹⁵) a lattice mismatch of ~16% can be calculated between the a and b parameter of tetragonal

* To whom correspondence should be addressed.

(1) Triboulet, R.; Perriere, J. *Prog. Cryst. Growth Charact. Mater.* **2003**, *47*, 65–138.

(2) Greene, L. E.; Law, M.; Goldberger, J.; Kim, F.; Johnson, J. C.; Zhang, Y.; Saykally, R. J.; Yang, P. *Angew. Chem., Int. Ed.* **2003**, *42*, 3031–3034.

(3) Goldberger, J.; Sirbully, D. J.; Law, M.; Yang, P. *J. Phys. Chem. B* **2005**, *109*, 9–14.

(4) Law, J. B. K.; Thong, J. T. L. *Appl. Phys. Lett.* **2006**, *88*, 13314/1–13314/3.

(5) Cheng, B.; Shi, W.; Russell-Tanner, J. M.; Zhang, L.; Samulski, E. T. *Inorg. Chem.* **2006**, *45*, 1208–1214.

(6) Morse, D. E. *Trends Biotechnol.* **1999**, *17*, 230–232.

(7) Sumerel, J. L.; Yang, W.; Kisailus, D.; Weaver, J. C.; Choi, J. H.; Morse, D. E. *Chem. Mater.* **2003**, *15*, 4804–4809.

(8) Kakiuchi, K.; Hosono, E.; Kimura, T.; Imai, H.; Fujihara, S. *J. Sol-Gel Sci. Technol.* **2006**, *39*, 63–72.

(9) Schwenzer, B.; Roth, K. M.; Gomm, J. R.; Murr, M.; Morse, D. E. *J. Mater. Chem.* **2006**, *16*, 401–407.

(10) Stählin, W.; Oswald, H. R. *Acta Crystallogr.* **1970**, *B26*, 860–863.

(11) Kisailus, D. J.; Schwenzer, B.; Gomm, J.; Weaver, J. C.; Morse, D. E. *J. Am. Chem. Soc.* **2006**, *128*, 10276–10280.

(12) O'Brien, P.; Saeed, T.; Knowles, J. *J. Mater. Chem.* **1996**, *6*, 1135–1139.

(13) Izaki, M.; Ohmi, T. *J. Electrochem. Soc.* **1997**, *144*, L3–L5.

(14) Yamabi, S.; Imai, H. *J. Mater. Chem.* **2002**, *12*, 3773–3778.

(15) JCPDS-file 00-046-1088.

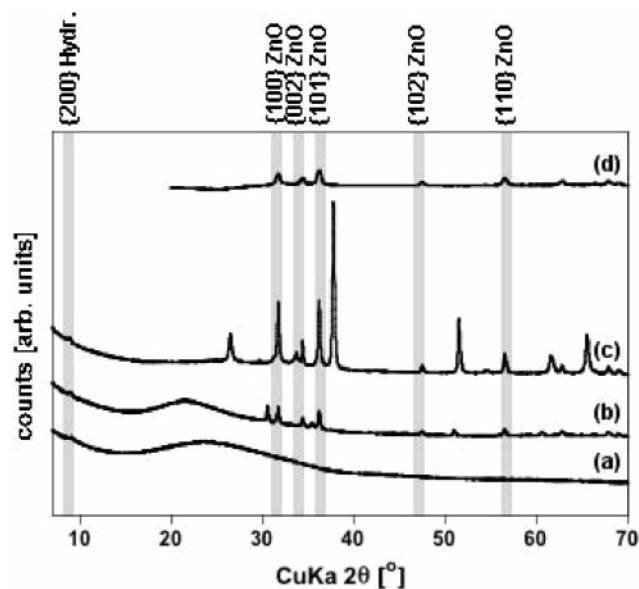


Figure 1. XRD pattern of thin films grown on different substrates from an aqueous 0.1 M $\text{Zn}(\text{NO}_3)_2$ solution by vapor-diffusion catalysis over the course of 6 h: (a) on amorphous glass, (b) on ITO coated glass, (c) on FTO coated glass, and (d) on (0001) face epitaxially grown ZnO. Indicated by gray bars are highest intensity peaks for $\text{Zn}_5(\text{OH})_8(\text{NO}_3)_2 \cdot 2\text{H}_2\text{O}$ ('Hydr.') and ZnO as respectively labeled. The peaks at 26° , 33° , 38° , 51° and above 60° in spectra b and c can be assigned to indium tin oxide (ITO).

SnO^{15} and the c parameter ($c = 5.517(0) \text{ \AA}^{10}$) of the monoclinic $\text{Zn}_5(\text{OH})_8(\text{NO}_3)_2 \cdot 2\text{H}_2\text{O}$ crystal structure. The calculated lattice mismatch of the c parameter of SnO^{12} with respect to hexagonal ZnO ($a = b = 3.23(0) \text{ \AA}^{16}$) is $<3\%$. The lattice mismatch between $\text{Zn}_5(\text{OH})_8(\text{NO}_3)_2 \cdot 2\text{H}_2\text{O}$ and the (0001) face of ZnO is $\sim 6\%$.

Figure 1 shows the X-ray diffraction (XRD) pattern of films grown from solution on the respective substrates during a 6 h exposure of the precursor solution to ammonia vapor at ambient temperature. An increase in crystallinity of the film is observed with increasing crystallinity of the underlying substrate; the signal/noise ratio in the XRD spectra increased, and for the thin films grown on FTO or ZnO substrates, no background elevation attributable to amorphous material was detectable. Furthermore, we observe a correlation between the preferred chemical composition of the as-prepared film and the underlying substrate. For the films grown on glass, ITO, and FTO, the 100% peak for $\text{Zn}_5(\text{OH})_8(\text{NO}_3)_2 \cdot 2\text{H}_2\text{O}$ at $d = 9.7 \text{ \AA}^{10}$ is visible. The films grown directly on glass exhibit the lowest crystallinity, and no signals indicating crystalline phases of other materials can be detected. We conclude from the relative intensities of the 100% peaks of $\text{Zn}_5(\text{OH})_8(\text{NO}_3)_2 \cdot 2\text{H}_2\text{O}$ and ZnO ($d = 9.7 \text{ \AA}^{10}$ and $d = 2.5 \text{ \AA}^{16}$ respectively) in spectra b and c that the as-grown films formed on ITO and FTO are predominantly composed of crystalline ZnO with some traces of crystalline $\text{Zn}_5(\text{OH})_8(\text{NO}_3)_2 \cdot 2\text{H}_2\text{O}$. For the film grown on epitaxial ZnO no traces of crystalline $\text{Zn}_5(\text{OH})_8(\text{NO}_3)_2 \cdot 2\text{H}_2\text{O}$ could be detected. An XRD spectrum of the material grown on epitaxial ZnO (Figure 1) was recorded with the sample tilted with respect to the X-ray beam to eliminate the otherwise dominant peak at $d = 2.5 \text{ \AA}^{16}$ that results from the underlying epitaxially grown substrate. (A control spectrum of the same sample recorded at normal orientation of the instrument stage was recorded for the range $2\theta = 7-70^\circ$ but is not shown here.) Only peaks that could be indexed to heterogeneously grown hexagonal ZnO were found for the film on the highly crystalline, epitaxially grown ZnO substrate; the peak at $d = 9.7 \text{ \AA}^{10}$ indicative

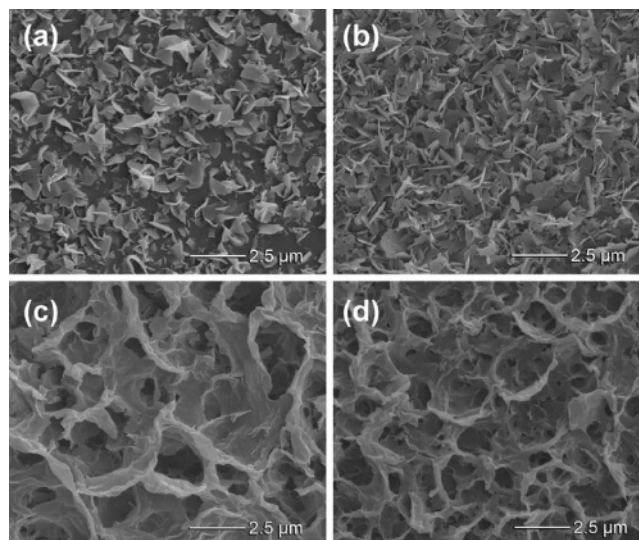


Figure 2. SEM images of thin films grown on different substrates from an aqueous 0.1 M $\text{Zn}(\text{NO}_3)_2$ solution by vapor-diffusion catalysis over the course of 6 h: (a) $\text{Zn}_5(\text{OH})_8(\text{NO}_3)_2 \cdot 2\text{H}_2\text{O}$ on amorphous glass, (b) a combination of $\text{Zn}_5(\text{OH})_8(\text{NO}_3)_2 \cdot 2\text{H}_2\text{O}$ and ZnO on ITO coated glass, (c) a combination of $\text{Zn}_5(\text{OH})_8(\text{NO}_3)_2 \cdot 2\text{H}_2\text{O}$ and ZnO on FTO coated glass, and (d) ZnO on the (0001) face of epitaxially grown ZnO.

of crystalline $\text{Zn}_5(\text{OH})_8(\text{NO}_3)_2 \cdot 2\text{H}_2\text{O}$ was not observed for this sample. (See the Supporting Information for details on the XRD experiments.) The crystalline correlation length within the deposited ZnO film is $\sim 3 \text{ nm}$. We attribute the differences in preferred crystal structure of the films prepared by vapor-diffusion catalysis on the different substrates to the differences in the number of possible nucleation sites provided and a progressively better lattice match for ZnO in the order of amorphous glass $<$ ITO \sim FTO $<$ ZnO.

Analysis by scanning electron microscopy (SEM) of the material grown on an amorphous glass substrate reveals thin, submicron-sized plates growing from an apparently continuous backplane (Figure 2a). The same morphology and habitus of the plates can be detected for the $\text{Zn}_5(\text{OH})_8(\text{NO}_3)_2 \cdot 2\text{H}_2\text{O}$ /ZnO grown on ITO (Figure 2b). However, the distance between the plates is smaller, and the density of the plates growing at an $\sim 90^\circ$ angle with respect to the substrate is higher, resulting in complete coverage of the backplane. The as-grown films on FTO (Figure 2c) and ZnO (Figure 2d) are noticeably different in appearance. By XRD, they are characterized as more crystalline and composed predominantly or entirely of ZnO instead of $\text{Zn}_5(\text{OH})_8(\text{NO}_3)_2 \cdot 2\text{H}_2\text{O}$. These differences are accompanied by a change in the nanostructure of the film. Individual plates are no longer visible; instead, a continuous layered network results from the nucleation on FTO or ZnO.

Having demonstrated these substrate-induced changes in thin film morphology, crystallinity, and composition compared to those previously reported for the unsupported, template-free $\text{Zn}_5(\text{OH})_8(\text{NO}_3)_2 \cdot 2\text{H}_2\text{O}$ films,⁹ we further analyzed the unsupported films that had grown at the air–water interface in the immediate vicinity surrounding the different substrates (see the Supporting Information). Although the film morphology was influenced by the proximity of the foreign substrates compared to the backplane/plate morphology of the previously described unsupported films, the chemical composition remained unchanged. In all cases, the unsupported films (adjacent to the exogenous substrates) were composed of pure $\text{Zn}_5(\text{OH})_8(\text{NO}_3)_2 \cdot 2\text{H}_2\text{O}$. Thus, we can conclude that the changes in chemical composition induced by the substrates do not extend to films grown around them. This is in agreement

with the understanding of the vapor-diffusion method indicating that the unsupported films form independently, either at the same time or prior to nucleation of material on the substrate.

Thickness measurements of the substrate-adherent films are in agreement with the observed XRD and SEM data. The $\text{Zn}_5(\text{OH})_8(\text{NO}_3)_2 \cdot 2\text{H}_2\text{O}$ film on glass is inhomogeneous in thickness, which can be explained by the observed island nucleation sites seen by SEM. On average, the plates protrude 1.4–1.8 μm from the backplane of the film. During the 6 h exposure to $\text{Zn}(\text{NO}_3)_2$ and catalyst, the film on ITO grew to a thickness of 100–200 nm, whereas on FTO, the predominantly ZnO film grew to a thickness of 200–300 nm. The submicron thickness of these films explains why the dominant peaks in the XRD patterns are those that can be indexed to the underlying SnO substrate. In contrast, the continuous 3-dimensional network of ZnO grown on the epitaxially oriented ZnO substrate is 1.4–1.9 μm thick. We attribute this increased thickness to the increased rate of nucleation as a result of the lattice matching between the product and the substrate.

3. Conclusion

In summary, we conclude that the vapor-diffusion catalysis method in combination with commercially available crystalline

substrates such as ITO coated glass, FTO coated glass, or epitaxially grown ZnO offers an alternative pathway to highly crystalline ZnO thin films with unique nanoscale features. These results further demonstrate the integrability of the kinetically controlled vapor-diffusion synthesis method into existing manufacturing processes such as MOCVD or MBE and extend its potential use as a low-cost alternative to these fabrication methods.

Acknowledgment. This work was supported in part by grants from the U.S. Department of Energy (DEFG03-02ER46006); DARPA (HR0011-04-1-0059); the U.S. Army Research Office through grant DAAD19-03-D-0004 to the Institute for Collaborative Biotechnologies; and the MRSEC Program (award No. DMR05-20415) of the National Science Foundation (UCSB Materials Research Laboratory).

Supporting Information Available: Details of the experimental procedures and additional characterization of unsupported Zn-containing films mentioned in this letter. This material is available free of charge via the Internet at <http://pubs.acs.org>.

LA0626914